AIAA JOURNAL
Vol. 30, No. 9, September 1992

Helicopter Rotor Blade Aeroelasticity in Forward Flight with an Implicit Structural Formulation

Roberto Celi*
University of Maryland, College Park, Maryland 20742

This paper describes an aeroelastic stability and response analysis in which the structural operator is formulated numerically, without expanding analytically the various algebraic expressions that make up the beam model. No ordering schemes need to be invoked to simplify the algebraic manipulations, and the various components of the mathematical model of the beam can be implemented and modified independently. The formulation is compatible with most solution algorithms. Two different implicit formulations are presented. The results of four illustrative examples are also presented. The first focuses on the effects of higher order kinematic nonlinearities on the aeroelastic stability and response of a hingeless rotor blade. The remaining three show how to introduce, using the implicit formulation, a nonlinear stress-strain relation in table look-up form, a composite cross section, and cross-sectional warping. Aeroelastic stability results are presented for all examples.

Nomenclature

A	= vector of aerodynamic loads formulated implicitly
C_T	= rotor thrust coefficient
EI_2, EI_3	= flap and lag bending stiffness
$\hat{e}_x, \hat{e}_y, \hat{e}_z$	= unit vectors of the undeformed blade coordinate system
$\hat{e}_x', \hat{e}_y', \hat{e}_z'$	= unit vectors of the deformed blade coordinate system
F_S^e	= element vector of nodal structural loads
GJ	= torsion stiffness
I	= vector of inertia loads formulated implicitly
l_e	= length of the eth finite element used to model the blade
M_F, M_L, M_T	= flap, lag, and torsion components of elastic moment
q	= state vector
R	= position vector of the generic point of the blade
S	= vector of structural loads formulated implicitly
S_{ij}	= component of the transformation matrix from undeformed to deformed blade coordinate system
T	= tension at a generic point of the blade
u	= elastic displacement of the cross section in the axial direction
v, w	= elastic displacements of the cross section in lag and flap bending, respectively
x	= spanwise coordinate of the blade
y	= vector of generalized coordinates of the blade
y_0, z_0	= cross-sectional coordinates
α	= vector of interpolation polynomials for modeling of axial degree of freedom
γ, η	= vector of interpolation polynomials for the modeling of bending
ϵ_{xx}, ϵ_{yy}, ϵ_{zz}, ϵ_{xy}, ϵ_{xz}, ϵ_{yz}	= strain components
θ_G	= total geometric pitch angle of the cross section
κ_y, κ_z	= blade curvatures
Λ	= ply angle of laminates for composite cross section
μ	= advance ratio
σ	= rotor solidity
σ_{xx}, σ_{yy}, σ_{zz}, τ_{xy}, τ_{xz}, τ_{yz}	= stress components
τ	= blade elastic twist
$[\Phi]$	= modal coordinate transformation matrix
$\boldsymbol{\phi}$	= vector of interpolation polynomials for the modeling of torsion
ϕ	= elastic rotation of the cross section in torsion
ψ	= blade azimuth angle
$(\ldots)_{,x}$	= $\partial(\ldots)/\partial x$
$(\overset{*}{\ldots})$	= $\partial(\ldots)/\partial\psi$

Introduction

In recent years there has been considerable interest in the development of advanced beam theories for rotary wing aeroelasticity applications. Two specific problems have been the focus of recent research in the field, namely the role of kinematic nonlinearities and that of nonclassical effects such as cross-sectional warping and transverse shear deformations. Beam theories capable of modeling the kinematic nonlinearities due to moderately large deflections have been available for over a decade.[1,2] These theories are based on the use of an ordering scheme to neglect systematically the large number of small, high-order nonlinear terms that arise in the derivation of the equations. Recent debate has focused on the desirability of including higher order nonlinearities, to relax the limitation that the deflections be only "moderately" large.[3] "Exact" theories that remove this limitation have also been proposed.[4–7] The interest in nonclassical effects is justified by the importance that these effects have for helicopter rotor blades built with advanced composite materials. A detailed review of the numerous research efforts in this area is beyond the scope of this paper. Detailed recent reviews have been published by Hodges[8] and Friedmann,[9] where extensive information on recent nonlinear beam theories can also be found.

Although these advanced beam theories are ultimately intended for application to rotorcraft dynamics and aeroelastic-

Received April 4, 1991; presented as Paper 91-1219 at the AIAA/ASME/ASCE/AHS/ASC 32nd Structures, Structural Dynamics, and Materials Conference, Baltimore, MD, April 8–10, 1991; revision received Dec. 14, 1991; accepted for publication Jan. 4, 1992.

*Assistant Professor, Center for Rotorcraft Education and Research, Department of Aerospace Engineering. Member AIAA.

ity, they have been actually incorporated in aeroelastic stability and response analyses only in a very small number of cases.[9] For example, with the partial exception of Ref. 10, no such theories appear to have been used for the calculation of the aeroelastic stability of a helicopter rotor in forward flight. One possible reason for this situation is that the incorporation of advanced beam theories in rotor aeroelastic codes requires a considerable implementation effort, to carry out all of the required software modifications. Another possible reason, especially for the treatment of nonlinearities, is that some of these theories are relatively complex and may require a substantial effort to be mastered and applied correctly to rotor aeroelasticity problems.

The main objective of this paper is to describe an aeroelastic stability and response analysis in which an implicit formulation is used for the structural operator. This formulation is called "implicit" because explicit algebraic expressions for the structural terms, as a function of the blade elastic displacements, are not needed. The various components of the beam theory, such as the coordinate transformation between the deformed and the undeformed blade coordinate systems, the strain-displacement relations, and the stress-strain relations, are implemented numerically and independently of one another. The implicit formulation of the structural operator is not a new beam theory, per se. However, as will be shown in the paper, when applied to an existing beam theory, it makes a large number of simplifying assumptions unnecessary. Then it may be argued that removing these assumptions is equivalent to formulating a new, more accurate version of that beam theory.

An additional objective of this paper is to present the results of four illustrative applications of the implicit formulation, namely, 1) an assessment of the effects of high-order kinematic nonlinearities, beyond those associated with moderate deflections, on the aeroelastic stability and response of a hingeless rotor in forward flight; 2) the introduction of a nonlinear shear stress-strain relationship, assumed to be available only in table look-up form; 3) the modeling of a blade spar built as a box beam made of composite materials; and 4) the introduction of cross-sectional warping in the mathematical model.

The implicit formulation has been successfully applied to the aerodynamic[11] and the inertia[12] operators of the rotary wing aeroelastic problem. The extension to the structural operator described in this paper results in an aeroelastic stability and response analysis formulated entirely in implicit form. This analysis, capable of modeling the behavior of the helicopter in straight or turning flight, can represent a useful research and development tool because individual portions of the various operators can be easily modified or replaced and because the blade model can be customized to a specific configuration with a relatively limited effort.

Problem Formulation

This section describes the treatment of the structural operator in the aeroelastic equations of motion of a helicopter rotor blade, using an implicit formulation technique. This operator is introduced in an aeroelastic stability and response analysis, capable of modeling helicopters in straight or turning flight, and described in detail in Refs. 13 and 14.

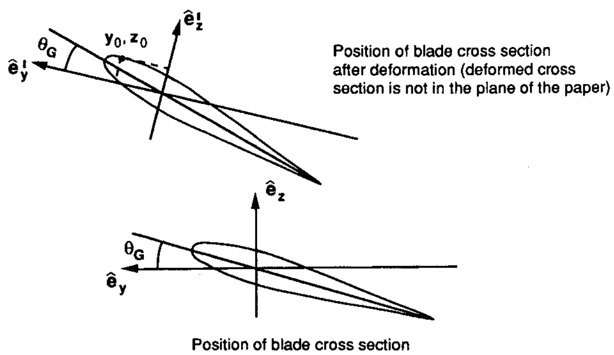

Fig. 1 Blade cross section and coordinate systems.

The implicit formulation represents a general framework that can, in principle, be applied to any beam theory. For illustration purposes, this section will focus on the application to isotropic, Bernoulli-Euler beams undergoing moderate deflections in coupled flap and lag bending and in torsion. The discussion that follows is based on assuming that the numerical value of the elastic displacements u, v, w, and ϕ, and of their derivatives with respect to space and time, are known as a function of the blade spanwise coordinate and azimuth angle. The geometry of the cross section of the blade and the coordinate systems used in the study are shown in Fig. 1.

Semi-Implicit Formulation

The simplest implementation of the implicit formulation is obtained by using directly the final expressions for the components of the elastic moment M acting on the blade cross section:

$$M = M_T\hat{e}_x + M_F\hat{e}_y + M_L\hat{e}_z \tag{1}$$

The components of M can be rewritten as:

$$M_T(v,\ w,\ \phi) = M_{t1} - M_{t0} \tag{2}$$

$$M_F(v,\ w,\ \phi) = M_{f2} - M_{f1} \tag{3}$$

$$M_L(v,\ w,\ \phi) = M_{l2} - M_{l1} \tag{4}$$

with

$$M_{t1} = GJ(\phi_{,x} + v_{,xx}w_{,x}) \tag{5}$$

$$M_{t0} = -\tfrac{1}{2}(EI_2 - EI_3)\sin 2\theta_G(v_{,xx}^2 - w_{,xx}^2) + (EI_2 - EI_3)\cos 2\theta_G(v_{,xx} + 2\phi w_{,xx}) \tag{6}$$

$$M_{f2} = (EI_2 - EI_3)\sin 2\theta_G(v_{,xx} + 2\phi w_{,xx}) + (EI_2 - EI_3)\cos 2\theta_G\phi v_{,xx} + (EI_2\sin^2\theta_G + EI_3\cos^2\theta_G)w_{,xx} \tag{7}$$

$$M_{f1} = GJ\phi_{,x}v_{,xx} + w_{,x}T \tag{8}$$

$$M_{l2} = (EI_2\cos^2\theta_G + EI_3\sin^2\theta_G)v_{,xx} + (EI_2 - EI_3)\sin 2\theta_G(w_{,xx} + 2\phi v_{,xx}) + (EI_2 - EI_3)\cos 2\theta_G\phi w_{,xx} \tag{9}$$

$$M_{l1} = GJ\phi_{,x}w_{,xx} + v_{,x}T \tag{10}$$

where the subscripts 2, 1, and 0 added to M_f, M_l, and M_t denote the portions of the structural operator that are integrated by parts twice, once, and not integrated, respectively, in the customary solution process. At this point a finite element discretization can be introduced, for example, using a Galerkin approach as described in Ref. 15. Then, after the appropriate number of integrations by parts is carried out, a vector of nodal structural loads can be defined as

$$F_S^e(\psi) = \int_0^{l_e}\begin{Bmatrix} M_{l2}\gamma_{,xx} + M_{l1}\gamma_{,x} \\ M_{f2}\eta_{,xx} + M_{f1}\eta_{,x} \\ M_{t1}\phi_{,x} + M_{t0}\phi \end{Bmatrix} dx \tag{11}$$

where γ, η, and ϕ are, respectively, the vectors of Hermite interpolation polynomials for lag bending, flap bending, and torsion. Only the numeric values of the integrand in Eq. (11) are required, not their analytical expressions. Therefore the numeric values of the components of $\boldsymbol{M}$, which can be calculated for any value of blade station and azimuth angle, can be directly introduced in Eq. (11).

Fully Implicit Formulation

The power and flexibility of the implicit formulation become clear when all of the portions of the beam theory are built numerically. This point will be illustrated by describing in detail the application to the beam theory of Rosen and Friedmann.[2] This theory is representative of the state of the art for hingeless rotor blades modeled as isotropic, Bernoulli-Euler beams undergoing small strains and moderate elastic deflections. The salient features of the derivation of Ref. 2 will be repeated here, with indications of the benefits of using an implicit approach.

A key ingredient for the formulation of the structural operator is the transformation between the triads of unit vectors that describe the undeformed and the deformed configuration of the beam. The coordinate transformation is given by

$$\begin{Bmatrix} \hat{e}_x' \\ \hat{e}_y' \\ \hat{e}_z' \end{Bmatrix} = \begin{bmatrix} S_{11} & S_{12} & S_{13} \\ S_{21} & S_{22} & S_{23} \\ S_{31} & S_{32} & S_{33} \end{bmatrix} \begin{Bmatrix} \hat{e}_x \\ \hat{e}_y \\ \hat{e}_z \end{Bmatrix} \tag{12}$$

where

$$S_{11} = \cos\theta_y \cos\theta_z$$

$$S_{12} = \cos\theta_y \sin\theta_z$$

$$S_{13} = -\sin\theta_y$$

$$S_{21} = \sin\theta_x \sin\theta_y \cos\theta_z - \cos\theta_x \sin\theta_z$$

$$S_{22} = \cos\theta_x \cos\theta_z + \sin\theta_x \sin\theta_y \sin\theta_z$$

$$S_{23} = \sin\theta_x \cos\theta_y$$

$$S_{31} = \cos\theta_x \sin\theta_y \cos\theta_z + \sin\theta_x \sin\theta_z$$

$$S_{32} = -(\sin\theta_x \cos\theta_z - \cos\theta_x \sin\theta_y \sin\theta_z)$$

$$S_{33} = \cos\theta_x \cos\theta_y$$

and where, furthermore, $\theta_x = \phi$ and

$$\begin{aligned} \sin\theta_y &= -\frac{w_{,x}}{\sqrt{1 + 2u_{,x} + u_{,x}^2 + v_{,x}^2 + w_{,x}^2}} \\ \cos\theta_y &= -\frac{\sqrt{1 + 2u_{,x} + u_{,x}^2 + v_{,x}^2}}{\sqrt{1 + 2u_{,x} + u_{,x}^2 + v_{,x}^2 + w_{,x}^2}} \\ \sin\theta_z &= -\frac{v_{,x}^2}{\sqrt{1 + 2u_{,x} + u_{,x}^2 + v_{,x}^2}} \\ \cos\theta_z &= -\frac{1 + u_{,x}}{\sqrt{1 + 2u_{,x} + u_{,x}^2 + v_{,x}^2}} \end{aligned} \tag{13}$$

The moderate deflection assumption is usually invoked at this point, to simplify the expressions for the elements of the coordinate transformation matrix $[S]$ by expanding the S_{ij} in truncated Taylor series. Thus the bending slopes $v_{,x}$ and $w_{,x}$ and the torsion deformation ϕ are assumed to be of order $\mathcal{O}(\epsilon)$, with $\epsilon \approx 0.2$, and the axial displacement u is assumed to be of order $\mathcal{O}(\epsilon^2)$. Furthermore, the assumption is made that quantities of order $\mathcal{O}(\epsilon^2)$ are negligible when compared with quantities of order $\mathcal{O}(1)$.

If the elastic displacements are assumed to be known, the element of $[S]$ can be calculated exactly, and neither assumptions on the size of the elastic displacements, nor ordering schemes, need to be invoked.

Another important ingredient consists of the curvatures κ_y and κ_z and twist τ, which are given by[2]

$$\begin{cases} \kappa_y = -\hat{e}_x' \cdot \hat{e}_{y,x}' = -(S_{11}S_{21,x} + S_{12}S_{22,x} + S_{13}S_{23,x}) \\ \kappa_z = -\hat{e}_x' \cdot \hat{e}_{z,x}' = -(S_{11}S_{31,x} + S_{12}S_{32,x} + S_{13}S_{33,x}) \\ \tau = -\hat{e}_y' \cdot \hat{e}_{y,x}' = -(S_{21}S_{21,x} + S_{22}S_{22,x} + S_{23}S_{23,x}) \end{cases} \tag{14}$$

At this point the assumption is made in Ref. 2 that $v_{,xx}$, $w_{,xx}$, and $\phi_{,x}$ are of similar magnitude, and the ordering scheme is applied. Once again, no such assumptions are required if an implicit approach is followed because the numeric values of the elements of $[S]$ are known. The derivatives of the elements of $[S]$ can be evaluated analytically, and the numeric values of the displacement quantities substituted into the resulting expressions.

The strain-displacement relations need to be defined next. If the Bernoulli-Euler assumption is used, the base vectors on the elastic axis of the deformed blade coincide with the $\hat{e}_x'$, $\hat{e}_y'$ and $\hat{e}_z'$ triad, and the position vector $\boldsymbol{R}$ of the generic point of the blade after deformation is given by[2]

$$\begin{aligned} \boldsymbol{R} = {} & (x_0 + u)\hat{e}_x + v_{,x}\hat{e}_y + w_{,x}\hat{e}_z + \tau\tilde{\varphi}(x_0, y_0, z_0, t)\hat{e}_x' \\ & + y_0\hat{e}_y' + z_0\hat{e}_z' \end{aligned} \tag{15}$$

where $\tilde{\varphi}(x_0, y_0, z_0, t)$ is a cross-sectional warping function. The strain components are given by

$$\begin{aligned} \epsilon_{xx} &= \tfrac{1}{2}(\boldsymbol{G}_x \cdot \boldsymbol{G}_x - 1) \\ \epsilon_{yy} &= \tfrac{1}{2}(\boldsymbol{G}_y \cdot \boldsymbol{G}_y - 1) \\ \epsilon_{zz} &= \tfrac{1}{2}(\boldsymbol{G}_z \cdot \boldsymbol{G}_z - 1) \\ \epsilon_{xy} &= \epsilon_{yx} = \tfrac{1}{2}(\boldsymbol{G}_x \cdot \boldsymbol{G}_y) \\ \epsilon_{xz} &= \epsilon_{zx} = \tfrac{1}{2}(\boldsymbol{G}_x \cdot \boldsymbol{G}_z) \\ \epsilon_{yz} &= \epsilon_{zy} = \tfrac{1}{2}(\boldsymbol{G}_y \cdot \boldsymbol{G}_z) \end{aligned} \tag{16}$$

where $\boldsymbol{G}_x = \boldsymbol{R}_{,x}$, $\boldsymbol{G}_y = \boldsymbol{R}_{,y}$, and $\boldsymbol{G}_z = \boldsymbol{R}_{,z}$. The assumption that the products of curvatures and twist by the cross-sectional coordinates y_0 and z_0 are of order less than $\mathcal{O}(\epsilon^2)$, invoked at this point in Ref. 2, is no longer required when the implicit approach is used. The vectors $\boldsymbol{G}$ should be written in terms of the cross-sectional coordinates, as shown here for $\boldsymbol{G}_x$:

$$\begin{aligned} \boldsymbol{G}_x = {} & (G_{x11} + G_{x21}y_0 + G_{x31}z_0)\hat{e}_x' + (G_{x12} + G_{x22}y_0 \\ & + G_{x32}z_0)\hat{e}_y' + (G_{x13} + G_{x23}y_0 + G_{x33}z_0)\hat{e}_z' \end{aligned} \tag{17}$$

where $G_{x11} = (1 + u_{,x})$, $G_{x21} = S_{21,x}$, $G_{x31} = S_{31,x}$, $G_{x23} = S_{23,x}$, $G_{x32} = S_{32,x}$, and $G_{x12} = G_{x22} = G_{x33} = 0$, and $\tilde{\varphi} \equiv 0$. When the implicit approach is used, each of the components ϵ of the strain vector should also be expressed in the form:

$$\epsilon = \epsilon_1 + \epsilon_2 y_0 + \epsilon_3 z_0 + \epsilon_4 y_0^2 + \epsilon_5 y_0 z_0 + \epsilon_6 z_0^2 \tag{18}$$

The generic stress-strain relation can now be written in matrix form as

$$\begin{Bmatrix} \sigma_{xx} \\ \sigma_{yy} \\ \sigma_{zz} \\ \tau_{xy} \\ \tau_{xz} \\ \tau_{yz} \end{Bmatrix} = [Q] \begin{Bmatrix} \epsilon_{xx} \\ \epsilon_{yy} \\ \epsilon_{zz} \\ \epsilon_{xy} \\ \epsilon_{xz} \\ \epsilon_{yz} \end{Bmatrix} \tag{19}$$

with each of the stress components expressed as shown in Eq. (18). For example,

$$\sigma = \sigma_1 + \sigma_2 y_0 + \sigma_3 z_0 + \sigma_4 y_0^2 + \sigma_5 y_0 z_0 + \sigma_6 z_0^2 \tag{20}$$

The calculation of stresses using Eq. (19) is carried out numerically at each radial station and azimuth angle of the blade, when the implicit approach is used. In that case, it is only necessary that the *numeric* value of the components of the matrix $[Q]$ be known. Therefore, it is quite simple to implement various stress-strain relationships that can describe, for example, nonlinear, viscoelastic, or hysteretic materials. It is also possible to use stress-strain relationships provided in table look-up form, such as those that may be determined through experimental tests.

The final ingredient of the beam theory is the stress-force relationship. Following Ref. 2, the structural force $\boldsymbol{F}$ and moment $\boldsymbol{M}$ acting on the cross section of the beam are given by

$$\boldsymbol{F} = T\hat{e}_x' + V_y\hat{e}_y' + V_z\hat{e}_z' = \int\int_A \boldsymbol{t}\, \mathrm{d}A \tag{21}$$

$$\boldsymbol{M} = M_x\hat{e}_x' + M_y\hat{e}_y' + M_z\hat{e}_z' = \int\int_A \boldsymbol{d} \times \boldsymbol{t}\, \mathrm{d}A \tag{22}$$

where

$$\boldsymbol{d} = \tau\tilde{\varphi}(x_0, y_0, z_0, t)\hat{e}_x' + y_0\hat{e}_y' + z_0\hat{e}_z' \tag{23}$$

$$\boldsymbol{t} = \sigma_{xx}\hat{e}_x' + \tau_{xy}\hat{e}_y' + \tau_{xz}\hat{e}_z' \tag{24}$$

Each component of the cross product should again be written as a polynomial in the cross-sectional coordinates y_0 and z_0. For example,

$$(\boldsymbol{d} \times \boldsymbol{t}) \cdot \hat{e}_x' = m_{x1} + m_{x2}y_0 + m_{x3}z_0 + m_{x4}y_0^2 + m_{x5}y_0z_0 + m_{x6}z_0^2 + m_{x7}y_0^3 + m_{x8}y_0^2z_0 + m_{x9}y_0z_0^2 + m_{x10}z_0^3 \tag{25}$$

Then each of the three moment components can be written in the following general form:

$$M_\alpha = \sum_{i=1}^{10} m_{\alpha i} I_i, \qquad \alpha = x,y,z \tag{26}$$

where

$$\begin{aligned} I_1 &= \textstyle\iint_A \mathrm{d}y_0\, \mathrm{d}z_0 \\ I_2 &= \textstyle\iint_A y_0\, \mathrm{d}y_0\, \mathrm{d}z_0 \\ I_3 &= \textstyle\iint_A z_0\, \mathrm{d}y_0\, \mathrm{d}z_0 \\ I_4 &= \textstyle\iint_A y_0^2\, \mathrm{d}y_0\, \mathrm{d}z_0 \\ I_5 &= \textstyle\iint_A y_0z_0\, \mathrm{d}y_0\, \mathrm{d}z_0 \\ I_6 &= \textstyle\iint_A z_0^2\, \mathrm{d}y_0\, \mathrm{d}z_0 \\ I_7 &= \textstyle\iint_A y_0^3\, \mathrm{d}y_0\, \mathrm{d}z_0 \\ I_8 &= \textstyle\iint_A y_0^2z_0\, \mathrm{d}y_0\, \mathrm{d}z_0 \\ I_9 &= \textstyle\iint_A y_0z_0^2\, \mathrm{d}y_0\, \mathrm{d}z_0 \\ I_{10} &= \textstyle\iint_A z_0^3\, \mathrm{d}y_0\, \mathrm{d}z_0 \end{aligned} \tag{27}$$

Each of the three force components can be expanded in a similar way.

As indicated in Eq. (22), the components of the structural moment $\boldsymbol{M}$ are expressed in the deformed coordinate system. Because the equations of motion of the blade are written in the undeformed coordinate system, the components of $\boldsymbol{M}$ must be transformed to this coordinate system. In Ref. 2, the transformation requires the use of the ordering scheme. Some additional assumptions concerning the relative magnitude of the blade stiffnesses in flap, lag, and torsion are invoked. When the implicit approach is used, no assumptions need to be invoked, and the transformation can be implemented exactly. Thus, the resulting structural operators associated with the axial, lag, flap, and torsion equations of motion, respectively, are

$$T_{,x} \tag{28}$$

$$[M_{z,x} + S_{13,x}M_x + (S_{23,x} - S_{13}S_{21,x})M_y - S_{32}M_{y,x}]_{,x} \tag{29}$$

$$[M_{y,x} + S_{12,x}M_x + (S_{32,x} - S_{12}S_{31,x})M_z - S_{23}M_{z,x}]_{,x} \tag{30}$$

$$M_{x,x} + (S_{21,x} + S_{13}S_{23,x})M_y + (S_{31,x} + S_{12}S_{32,x})M_z \tag{31}$$

After the appropriate number of integrations by parts is carried out, a vector of nodal structural loads can be defined as:

$$\boldsymbol{F}_S^e(\psi) = \int_0^{l_e} \begin{Bmatrix} T_1\boldsymbol{\alpha}_{,x} \\ M_{l2}\boldsymbol{\gamma}_{,xx} + m_{l1}\boldsymbol{\gamma}_{,x} \\ M_{f2}\boldsymbol{\eta}_{,xx} + M_{f1}\boldsymbol{\eta}_{,x} \\ M_{t1}\boldsymbol{\phi}_{,x} + M_{t0}\boldsymbol{\phi} \end{Bmatrix} \mathrm{d}x \tag{32}$$

in which

$$T_1 = T \tag{33}$$

$$M_{l2} = M_z - S_{32}M_y \tag{34}$$

$$M_{l1} = -S_{13,x}M_x - (S_{23,x} - S_{13}S_{21,x})M_y - S_{32,x}M_y \tag{35}$$

$$M_{f2} = -(M_y - S_{23}M_z) \tag{36}$$

$$M_{f1} = S_{12,x}M_x + (S_{32,x} - S_{12}S_{31,x})M_y + S_{23,x}M_y \tag{37}$$

$$M_{t1} = M_x \tag{38}$$

$$M_{t0} = (S_{21,x} + S_{13}S_{23,x})M_y + (S_{31,x} + S_{12}S_{32,x})M_z \tag{39}$$

Solution Technique

The results presented in this paper have been obtained by solving the aeroelastic stability and response problem using a quasilinearization solution algorithm. The equations of motion can be written in first-order form as follows:

$$\begin{aligned} \mathring{\boldsymbol{q}}(\psi) &= \boldsymbol{A}(\boldsymbol{q},\mathring{\boldsymbol{q}};\psi) + \boldsymbol{I}(\boldsymbol{q},\mathring{\boldsymbol{q}};\psi) + \boldsymbol{S}(\boldsymbol{q},\mathring{\boldsymbol{q}};\psi) \\ &= \boldsymbol{F}_{NL}(\boldsymbol{q},\mathring{\boldsymbol{q}};\psi) \end{aligned} \tag{40}$$

The vectors $\boldsymbol{A}$, $\boldsymbol{I}$, and $\boldsymbol{S}$ contain, respectively, the aerodynamic, inertia, and structural contributions. The numerical value of these vectors for given values of $\boldsymbol{q}$, $\mathring{\boldsymbol{q}}$, and ψ is known. Their explicit algebraic forms are not known.

Let $\boldsymbol{q}^k(\psi)$ be an approximate solution of Eq. (40). Quasilinearization is based on performing a first-order Taylor series expansion of Eq. (40) about $\boldsymbol{q}^k$:

$$\mathring{\boldsymbol{q}}^{k+1} = \mathring{\boldsymbol{q}}^k + \left[\frac{\partial \boldsymbol{F}_{NL}}{\partial \boldsymbol{q}}\right](\boldsymbol{q}^{k+1} - \boldsymbol{q}^k) + \left[\frac{\partial \boldsymbol{F}_{NL}}{\partial \mathring{\boldsymbol{q}}}\right](\mathring{\boldsymbol{q}}^{k+1} - \mathring{\boldsymbol{q}}) \tag{41}$$

in which

$$\left[\frac{\partial \boldsymbol{F}_{NL}}{\partial \boldsymbol{q}}\right]^k = \left[\frac{\partial \boldsymbol{A}}{\partial \boldsymbol{q}}\right]^k + \left[\frac{\partial \boldsymbol{I}}{\partial \boldsymbol{q}}\right]^k + \left[\frac{\partial \boldsymbol{S}}{\partial \boldsymbol{q}}\right]^k$$

$$\left[\frac{\partial \boldsymbol{F}_{NL}}{\partial \mathring{\boldsymbol{q}}}\right]^k = \left[\frac{\partial \boldsymbol{A}}{\partial \mathring{\boldsymbol{q}}}\right]^k + \left[\frac{\partial \boldsymbol{I}}{\partial \mathring{\boldsymbol{q}}}\right]^k + \left[\frac{\partial \boldsymbol{S}}{\partial \mathring{\boldsymbol{q}}}\right]^k$$

Eq. (41) can be written in the form

$$\mathring{q}^{k+1} = B^k(\psi)q^{k+1} + f^k(\psi) \tag{42}$$

Comparing Eqs. (41) and (42), one has

$$B^k(\psi) = \left([I] - \left[\frac{\partial F_{NL}}{\partial \mathring{q}}\right]^k\right)^{-1}\left[\frac{\partial F_{NL}}{\partial q}\right]^k \tag{43}$$

$$f^k(\psi) = \left([I] - \left[\frac{\partial F_{NL}}{\partial \mathring{q}}\right]^k\right)^{-1}\left(\mathring{q}^k - \left[\frac{\partial F_{NL}}{\partial q}\right]^k q^k - \left[\frac{\partial F_{NL}}{\partial \mathring{q}}\right]^k \mathring{q}^k\right) \tag{44}$$

Further details of the solution process, including the calculation of the Floquet transition matrix at the end of one period, and the determination of initial conditions for Eq. (42) can be found in Ref. 11. The treatment of the structural terms will be shown here in detail.

The state vector $q(\psi)$ is defined as

$$q(\psi) = \begin{Bmatrix} y(\psi) \\ \mathring{y}(\psi) \end{Bmatrix} \tag{45}$$

where $y(\psi)$ is the vector of generalized coordinates for the blade, which is related to the vector y_N of nodal degrees of freedom by

$$y_N = [\Phi]y \tag{46}$$

The generic term ϕ_{ij} of the modal coordinate transformation matrix $[\Phi]$ represents the generalized displacement of the ith nodal degree of freedom in the jth coupled normal mode of the blade. Thus, once q^k and $\mathring{q}^k$ are known, the vectors y_N, $\mathring{y}_N$, and $\mathring{\mathring{y}}_N$ can be obtained using Eqs. (45) and (46), from which the elastic displacements at any blade station x can be recovered. For example, the lag bending displacement v is given by:

$$v(x, \psi) = v_1(\psi)H_1(x) + v_{,x1}(\psi)H_2(x) + v_2(\psi)H_3(x) + v_{,x2}(\psi)H_4(x) \tag{47}$$

where v_1, $v_{,x1}$, v_2, and $v_{,x2}$ are components of the vector y_N and represent, respectively, the displacements and slopes at the inboard and outboard node of the element, and the $H_j(x)$ are Hermite interpolation polynomials. Equation (47) can be differentiated as required to obtain the space and time derivatives of v. Thus, given the state vector $q^k(\psi)$ it is possible to calculate the elastic displacements of the blade, and their space and time derivatives, that are required to implement the implicit formulation of the structural operator.

The vector $S(q, \mathring{q}; \psi)$ of structural loads in Eq. (40) is given by

$$S(q, \mathring{q}; \psi) = \sum_{e=1}^{N} [\Phi]^e F_S^e \tag{48}$$

in which $[\Phi]^e$ is the portion of the modal coordinate transformation matrix $[\Phi]$ that contains the nodal degrees of freedom of the eth element, F_S^e is the structural load vector, defined as in Eq. (11) or Eq. (32), and the summation extends over the N finite elements used to model the blade. Therefore, Eq. (48) provides simultaneously the modal coordinate transformation and the assembly procedure for the N element vectors.

Finally, the derivative matrices $[\partial S/\partial q]^k$ and $[\partial S/\partial \mathring{q}]^k$ have the form

$$\left[\frac{\partial S}{\partial q}\right]^k = \begin{bmatrix} 0 & 0 \\ \left[\frac{\partial S}{\partial y}\right]^k & \left[\frac{\partial S}{\partial \mathring{\mathring{y}}}\right]^k \end{bmatrix} \tag{49}$$

$$\left[\frac{\partial S}{\partial \mathring{q}}\right]^k = \begin{bmatrix} 0 & 0 \\ 0 & \left[\frac{\partial S}{\partial \mathring{y}}\right]^k \end{bmatrix} \tag{50}$$

The derivative matrices are computed numerically, using finite difference approximations.

It should be emphasized that using the results of the kth iteration to build the vectors and matrices required to perform the $k + 1$th iteration does not introduce any approximations, except for those inherent in numerical differentiation. In other words, the implicit approach to the formulation of the aeroelastic equations of motion does not introduce any approximations compared with the case in which explicit algebraic expansions are carried out. This is evident from Eq. (42): in fact, the matrix $B^k(\psi)$ and the vector $f^k(\psi)$, required to obtain the $k + 1$th approximation $\mathring{q}^{k+1}$, are built, whether explicitly or implicitly, based on the results on the kth iteration.

This result is not limited to quasilinearization and can be extended to all Newton-based solution techniques. In fact, Eq. (42) is a special version of the more general Newton iteration equation[16]:

$$x_1 = x_0 - [P'(x_0)]^{-1}P(x_0) \tag{51}$$

The operator P is a differential operator in the case of quasilinearization or an algebraic operator when the solution of the aeroelastic equations of motion is reduced to the solution of a set of nonlinear algebraic equations. This is the case when Galerkin's method, harmonic balance, or the finite element in time method are used. Therefore, an implicit formulation is compatible with all these methods.

This formulation is also compatible with direct numerical integration solution techniques. An ordinary differential equation (ODE) solver has the following general form:

$$q(\psi_{n+1}) = q(\psi_n) + F[q(\psi_n), \Delta\psi; \psi] \tag{52}$$

in which F is a function of the right-hand side of the system of ODE and $\Delta\psi$ is the step size. The function F depends on the state at the nondimensional time ψ_n, and perhaps at previous times ψ_{n-1}, ψ_{n-2}, etc. All of these state vectors are known.

Results

The purpose of this section is to present four illustrative examples of application of the implicit beam formulation to aeroelastic stability and response problems. The baseline rotor blade configuration used in the calculations is a hingeless blade with fundamental natural frequencies in lag, flap, and torsion of 0.73, 1.12, and 3.17/rev, respectively. The thrust coefficient is $C_T = 0.005$, the solidity is $\sigma = 0.07$.

To maintain consistency with Refs. 11 and 12, the results were obtained using a mathematical model that did not include the axial equation and the axial degree of freedom. Thus the axial degree of freedom u was eliminated by assuming that the blade was inextensional, and the tension T was given by

$$T = \int_x^1 p_{,x}\, dx \tag{53}$$

in which $p_{,x}$ is the distributed applied force in the $\hat{e}_x$ direction, and x is the spanwise blade coordinate.

To validate the solution procedure of the present formulation, the results obtained using the semi-implicit formulation were compared with those obtained using the conventional, explicit formulation of the structural operator of Ref. 11. The theory is identical in both formulations, and the possible source of discrepancy was the fact that the derivative matrices in Eqs. (49) and (50) were calculated analytically, and therefore exactly, when the explicit formulation was used. The agreement between the two sets of results was excellent, with the relative differences in blade response and stability eigenvalues consistently less than 0.01%. The required CPU time varies depending on several factors, such as the advance ratio, the complexity of the aerodynamic model, or the number of steps that the variable step variable order ODE solver requires. For $\mu \leq 0.3$, and when stall and compressibility effects are neglected, each iteration of quasilinearization requires about 200 s of CPU time for the explicit formulation of the structural operator, about 230 s for the semi-implicit formulation, and about 250 s for the fully implicit formulation. All of the CPU times refer to an IBM 3081D computer. The solution of all of the stability problems presented in this paper required two or three iterations of quasilinearization. The algorithm converged in all cases.

Example I—Effect of Kinematic Nonlinearities

The effect of kinematic nonlinearities was studied by comparing results obtained using the semi-implicit and the fully implicit formulations of the structural operator described in the previous sections. The former is essentially based on the assumption that the elastic slopes in bending and the torsional deformations are of order $\mathcal{O}(\epsilon)$ and that terms of order $\mathcal{O}(\epsilon^2)$ are negligible compared with terms of order $\mathcal{O}(1)$. No such assumption is explicitly invoked in the latter.

Table 1 shows the real parts of the characteristic exponents for the six lowest frequency blade modes, obtained using the semi-implicit and the fully implicit formulation of the structural operator outlined in this paper. The results refer to the baseline blade configuration. It is evident from the table that the largest discrepancy is of less than 1%. Figure 2 shows the blade tip response in flap, lag, and torsion at an advance ratio $\mu = 0.4$ calculated using the two formulations. Again, the differences are extremely small and barely noticeable in the scale of the figure.

These results suggest that including additional high-order nonlinear kinematic terms in theories such as those of Refs. 1 and 2 produces very small changes in the results. It should be emphasized, however, that an implicit formulation of a moderate deflection beam theory will not automatically transform it into an arbitrarily large deflection beam theory. Kinematic and stress-strain relations may have to be appropriately modified for this purpose.

Table 1 Comparison of real parts of the characteristic exponents for the six lowest frequency coupled rotor modes using the semi-implicit and the fully implicit formulation, soft-in-plane blade; $C_T/\sigma = 0.071$.

Advance ratio	Semi-implicit	Fully implicit	Relative change, %
	First lag		
0.1	−0.013045	−0.01302	0.19
0.2	−0.011895	−0.011875	0.17
0.3	−0.0090614	−0.0090454	0.18
	Second lag		
0.1	−0.0039019	−0.0038676	0.89
0.2	−0.0051939	−0.0051526	0.80
0.3	−0.023644	−0.23444	0.85
	First torsion		
0.1	−0.29369	−0.29237	0.45
0.2	−0.29304	−0.29188	0.40
0.3	−0.29209	−0.29209	0.00
	First flap		
0.1	−0.35864	−0.35883	−0.05
0.2	−0.36156	−0.36172	−0.04
0.3	−0.37928	−0.37948	−0.05
	Second flap		
0.1	−0.28435	−0.28565	−0.46
0.2	−0.28664	−0.28783	−0.41
0.3	−0.27904	−0.28014	−0.39
	Third flap		
0.1	−0.24719	−0.24713	0.02
0.2	−0.24869	−0.24861	0.03
0.3	−0.25159	−0.25153	0.02

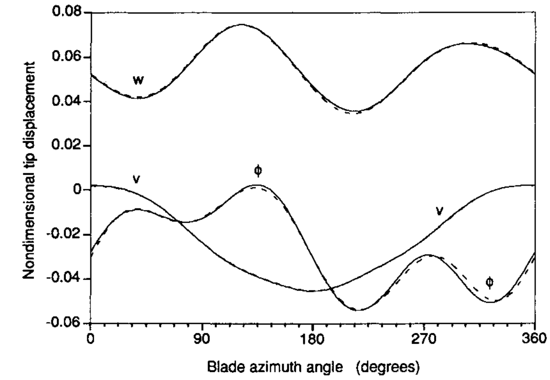

Fig. 2 Comparison of rotor blade responses obtained using semi-implicit and fully implicit formulation, soft-in-plane blade configuration; $\mu = 0.4$, $C_T = 0.005$, and $\sigma = 0.07$.

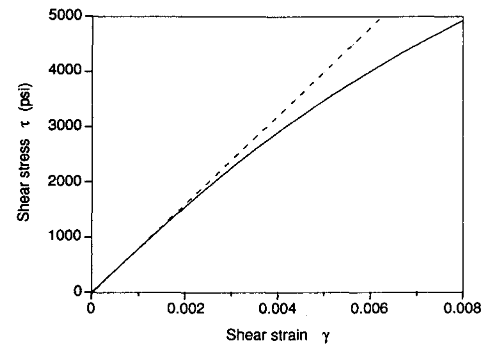

Fig. 3 Linear and nonlinear shear stress-strain curves.

It should also be pointed out that, as stated in Ref. 9, all of the components of a mathematical model for rotary wing aeroelasticity should be of comparable accuracy. Therefore, an excessive preoccupation with high-order kinematic nonlinearities is not justified unless, for example, the aerodynamic model can provide a similar degree of accuracy.[9]

Example II—Nonlinear Shear Stress-Strain Relationship

Results were obtained for a blade built of a hypothetical material having the following nonlinear shear stress-strain relationship:

$$\epsilon_{xy} = S_1\tau_{xy} + S_2\tau_{xy}^3 \tag{54}$$

$$\epsilon_{xz} = S_1\tau_{xz} + S_2\tau_{xz}^3 \tag{55}$$

The values chosen for the constants are $S_1 = 0.125 \times 10^{-5}$ (psi)$^{-1}$ and $S_2 = 1.53 \times 10^{-14}$ (psi)$^{-3}$, resulting in material characteristics in shear that resemble those of certain boron-epoxy composites.[17] The stress-strain curve described by Eqs. (54) and (55) is shown in Fig. 3.

It should be noted that in Eq. (19) the stresses, rather than the strains, are required. Therefore, Eqs. (54) and (55) should be seen as cubic equations in τ_{xy} and τ_{xz}. Of the three solutions of each of the cubic equations, only one is real and should be used in Eq. (19). Rather than solving two nonlinear equations at each blade radial station and azimuth angle, the $\tau(\epsilon)$ relationships were implemented in table look-up form. A table of $\tau(\epsilon)$ pairs was calculated using Eqs. (54) and (55), and linear interpolation was used to obtain the required τ. Thus this example clearly shows the flexibility provided by the implicit formulation, in which explicit functional expressions are not required.

Table 2 shows the real parts of the characteristic exponents for the six lowest frequency modes obtained using a linear stress-strain relationship, obtained by neglecting the cubic

Table 2 Comparison of real parts of the characteristic exponents for the six lowest frequency coupled rotor modes using the linear and the nonlinear $\tau(\epsilon)$ relationships; $C_T/\sigma = 0.071$.

Relative Mode	Linear	Nonlinear	Change, %
First lag	−0.055824	−0.0546796	−2.05
Second lag	−0.038672	−0.0391167	1.15
First torsion	−0.27727	−0.2723623	−1.77
First flap	−0.37647	−0.3748512	−0.43
	−0.28175	−0.2823135	0.20
Second flap	−0.21334	−0.2149827	0.77
Third flap	−0.22113	−0.2211521	0.01

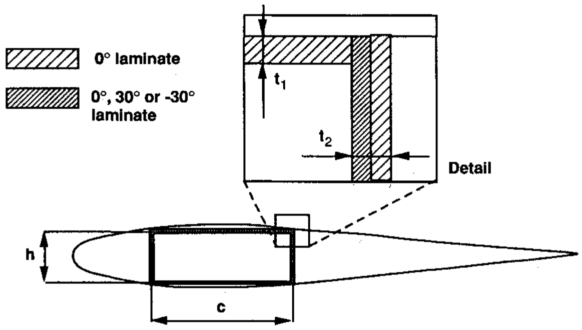

Fig. 4 Geometry of the composite blade cross section.

terms in Eqs. (54) and (55), and the nonlinear relationship. These results suggest that material nonlinearities of the type and the strength used in this example should play a minor role in the aeroelastic stability and response characteristics of the blade. It should be kept in mind, however, that Bernoulli-Euler hypothesis contains a well known inconsistency in the treatment of the shear stresses and strains (see page 50 of Ref. 2). Therefore, the effects of material nonlinearities may not be modeled accurately by the theory used in this example.

Example III—Composite Rotor Blade

An implicit formulation of the structural operator can help reduce the effort required to model rotor blades made of composite material. In this example the load carrying portion of the blade is modeled as a box beam, as shown in Fig. 4. The top flanges of the spar have a zero ply angle. The laminates making up the outer half of the side flanges also have a zero ply angle. The ply angle of the inner half of the side flanges is equal to Λ. This cross section is identical to the case I cross section of Ref. 10. The blade properties were determined so as to be identical to the baseline blade when the ply angles of all laminates are equal to zero. The normal modes calculated for the $\Lambda = 0$ deg configuration were also used for the nonzero Λ cases.

For isotropic beams the stress-strain relation, Eq. (19), is simply implemented as

$$\sigma_{xx} = E\epsilon_{xx}$$
$$\tau_{xy} = G\epsilon_{xy} \tag{56}$$
$$\tau_{xz} = G\epsilon_{xz}$$

For the composite cross section, on the other hand, the following stress-strain relations are used for the kth lamina of the horizontal flanges[10]:

$$\sigma^k_{xx} = \bar{Q}^k_{11}\epsilon_{xx} + \bar{Q}^k_{16}\epsilon_{xy}$$
$$\tau^k_{xy} = \bar{Q}^k_{16}\epsilon_{xx} + \bar{Q}^k_{66}\epsilon_{xy} \tag{57}$$
$$\tau^k_{xz} = 0$$

and for the lth lamina of the vertical flanges[10]:

$$\sigma^l_{xx} = \bar{Q}^l_{11}\epsilon_{xx} + \bar{Q}^l_{16}\epsilon_{xy}$$
$$\tau^l_{xy} = 0 \tag{58}$$
$$\tau^l_{xz} = \bar{Q}^l_{16}\epsilon_{xx} + \bar{Q}^l_{66}\epsilon_{xz}$$

Because the cross section is no longer isotropic, Eq. (22) needs to be slightly modified as

$$M = M_x\hat{e}_x' + M_y\hat{e}_y' + M_z\hat{e}_z' = \sum_j \int\int_{A_j} d \times t_j \, dA \tag{59}$$

with

$$t_j = \sigma^j_{xx}\hat{e}_x' + \tau^j_{xy}\hat{e}_y' + \tau^j_{xz}\hat{e}_z' \tag{60}$$

in which the index j indicates each of the various portions of which the cross section is composed. Equation (26) is then rewritten as

$$M_\alpha = \sum_j \sum_{i=1}^{10} m^j_{\alpha i} I^j_i \, dA\,, \qquad \alpha = x,y,z \tag{61}$$

in which the integrals I^i_j are calculated over the jth portion of the cross section. Thus, only the simple bookkeeping modifications of Eqs. (59–61) are required to implement the stress-strain relations of Eqs. (57) and (58). It should be emphasized, however, that additional ingredients may be required for an accurate mathematical model of a composite rotor blade, beyond those included here. For example, a detailed modeling of cross-sectional warping is often required for composite blades.[8–10]

The stability of the first and second lag modes are shown by the solid lines in Figs. 5 and 6, respectively, as a function of the advance ratio μ, for three different values of the ply angle Λ of the inner half of the vertical flanges of the cross section. The ply angle Λ is positive if the fibers are oriented toward the top flange. The figures show that for $\Lambda = 30$ deg the first lag mode is unstable for all values of μ. A ply angle $\Lambda = -30$ deg, on the other hand, is generally stabilizing. These trends are the same as those identified in Ref. 10. The stability of the second lag mode increased for both configurations with nonzero Λ. The CPU time required for each iteration of quasilinearization was of about 300–320 s.

A fully implicit formulation simplifies the treatment of the structural operator because the implementation of the beam theory is modular, and each element of the theory can be modified independently from the others. It can be argued, however, that some of the physical interpretation may be lost in the process. For example, in Ref. 10, a complete explicit expansion of the structural operator leads to the identification

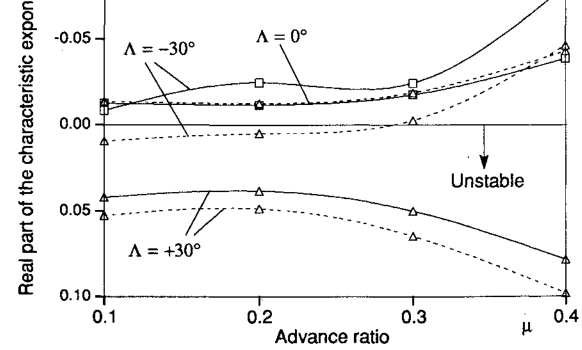

Fig. 5 Stability of the first lag mode: solid lines; no warping model; dashed lines, with warping model; $C_T = 0.005$, and $\sigma = 0.07$.

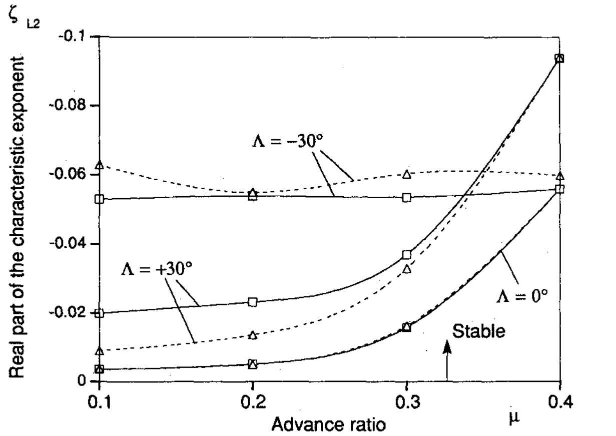

Fig. 6 Stability of the second lag mode: solid lines; no warping model; dashed lines, with warping model; $C_T = 0.005$, and $\sigma = 0.07$.

of stiffness coupling parameters that are shown to be similar to the traditional pitch-flap or pitch-lag coupling parameters and that help explain the effects of ply angle on the aeroelastic stability and response of the blade. On the other hand, if a fully implicit formulation is used, such an identification is not possible. Therefore, it may still be worthwhile to carry out explicit algebraic expansions of structural terms, especially in research-type applications, possibly in the context of the semi-implicit formulation outlined in the previous section of this paper.

Example IV—Treatment of Cross-Sectional Warping

Especially for blades made of composite materials, the model should include cross-sectional warping and other non-classical effects. The additional terms can be handled in a particularly simple manner if they can be expressed as polynomials in the cross-sectional dimensions y_0 and z_0. For example, if the following simple expression for cross-sectional warping is used,[10]

$$\tilde{\varphi} = \beta y_0 z_0 \tag{62}$$

with

$$\beta = \text{const} = \frac{ct_2 - ht_1}{ct_2 - ht_1} \tag{63}$$

(all of the cross-sectional dimensions are defined in Fig. 4), then Eq. (17) only needs to be modified to include the additional underlined terms:

$$\begin{aligned} G_x = {} & (G_{x11} + G_{x21}y_0 + G_{x31}z_0 + \underline{G_{x51}y_0z_0})\hat{e}_x' \\ & + (G_{x12} + G_{x22}y_0 + G_{x32}z_0 + \underline{G_{x52}y_0z_0})\hat{e}_y' \\ & + (G_{x13} + G_{x23}y_0 + G_{x33}z_0 + \underline{G_{x53}y_0z_0})\hat{e}_z' \end{aligned} \tag{64}$$

where the additional terms are $G_{x51} = \tau_{,x}\beta$, $G_{x52} = \tau\beta\kappa_y$, and $G_{x53} = \tau\beta\kappa_z$. No changes are required in the polynomial expressions for G_y and G_z; the term $\tau\beta$ has to be added to G_{y31} and G_{z21}. A term $\tau\beta y_0 z_0$ also needs to be added to the $\hat{e}_x'$ component of the vector $\boldsymbol{d}$.

With the exception of some bookkeeping modifications to account for the extra terms in y_0 and z_0, no further changes are required in the implementation of the theory to account for warping as defined by Eq. (62).

Figure 5 presents a comparison of the stability results for the first lag mode obtained with and without the modeling of warping, shown by the dashed and the solid lines, respectively. The same comparison for the second lag mode is presented in Fig. 6. Warping appears to have a negligible effect on the stability of the $\Lambda = 0$ deg configuration. The effect on the $\Lambda = 30$ deg configuration is destabilizing for both lag modes; the general qualitative behavior with respect to μ remains unchanged. Warping is destabilizing for the $\Lambda = -30$ deg configuration, to the point that the first lag mode becomes unstable. No such instability was observed in Ref. 10. Possible reasons for the differences may be the different cross-sectional characteristics (the blade of Ref. 10 has a fundamental frequency of 4.41/rev) or the fact that the normal modes used in the present example do not include the structural coupling effects introduced by nonzero ply angles. The CPU time required for each iteration of quasilinearization was about 320–340 s.

Conclusions

This paper describes an aeroelastic analysis with an implicit formulation of the structural operator. The various components of the structural model are implemented numerically and independently. No ordering schemes are required, and no limitations need to be placed on the order of magnitude of the elastic deformations, to simplify the subsequent algebraic manipulations. Therefore, it is possible to increase the accuracy of traditional moderate deflection beam theories through implicit formulations and without having to resort to complex results of solid mechanics.

As far as the treatment of geometrically nonlinear terms is concerned, including additional higher order nonlinearities to moderate deflection beam theories produces minimal changes in the aeroelastic stability and response results. Therefore, the most important contribution of the implicit formulation described in this paper is not the ability to include additional nonlinear terms. Rather, the usefulness lies in the flexibility and modularity that this formulation allows.

The illustrative examples presented in the paper show that such diverse items as a nonlinear stress-strain relationship in table look-up form, a structural cross section made of composite materials, and cross-sectional warping can be implemented with a limited effort and only a modest penalty in computational requirements. Therefore, the implicit formulation presented in this paper may represent a useful tool and reduce considerably the time required to incorporate new blade modeling theories in practical aeroelastic stability and response computer codes.

Acknowledgments

This work was supported by the Army Research Office, Contract DAAL-03-88-C-002, technical monitors were Robert Singleton and Tom Doligalski.

References

[1]Hodges, D. H., and Dowell, E. H., "Nonlinear Equations of Motion for the Elastic Bending and Torsion of Twisted Non-Uniform Blades," NASA TN-D 7818, 1974.

[2]Rosen, A., and Friedmann, P. P., "Nonlinear Equations of Equilibrium for Elastic Helicopter or Wind Turbine Blades Undergoing Moderate Deflections," NASA CR-159478, Dec. 1978.

[3]Mathew, M. B., and Loewy, R. B., "Nonlinear Effects in Helicopter Rotor Forward Flight Forced Response," *Vertica*, Vol. 14, No. 1, 1990, pp. 1–18.

[4]Crespo da Silva, M. R. M., and Hodges, D. H., "Nonlinear Flexure and Torsion of Rotating Beams, with Application to Helicopter Rotor Blades—I. Formulation," *Vertica*, Vol. 10, No. 2, 1986, pp. 151–169.

[5]Crespo da Silva, M. R. M., and Hodges, D. H., "Nonlinear Flexure and Torsion of Rotating Beams, with Application to Helicopter Rotor Blades—II. Results for Hover," *Vertica*, Vol. 10, No. 2, 1986, pp. 171–186.

[6]Atilgan, A. R., and Hodges, D. H., "Nonlinear Beam Kinematics by Decomposition of the Rotation Tensor," *Journal of Applied Mechanics*, Vol. 54, No. 2, Feb. 1987, pp. 561–565.

[7]Hodges, D. H., "A Mixed Variational Formulation Based on Exact Intrinsic Equations for Dynamics of Moving Beams," *International Journal of Solids and Structures*, Vol. 26, No. 11, 1990, pp. 1253–1273.

[8] Hodges, D. H., "Review of Composite Beam Modeling," *AIAA Journal*, Vol. 28, No. 3, 1990, pp. 561-565.

[9] Friedmann, P. P., "Helicopter Rotor Dynamics and Aeroelasticity: Some Key Ideas and Insights," *Vertica*, Vol. 14, No. 1, 1990, pp. 101-121.

[10] Panda, B., and Chopra, I., "Dynamics of Composite Rotor Blades in Forward Flight," *Vertica*, Vol. 11, No. 1/2, 1987, pp. 187-209.

[11] Celi, R., and Friedmann, P. P., "Rotor Blade Aeroelasticity in Forward Flight with an Implicit Aerodynamic Formulation," *AIAA Journal*, Vol. 26, No. 12, 1988, pp. 1425-1433.

[12] Celi, R., "Effect of Hingeless Rotor Aeroelasticity on Helicopter Longitudinal Flight Dynamics," *Journal of the American Helicopter Society*, Vol. 36, No. 1, 1991, pp. 35-44.

[13] Celi, R., "Hingeless Rotor Dynamics in Coordinated Turns," *Journal of the American Helicopter Society*, Vol. 36, No. 4, Oct. 1991, pp. 39-47.

[14] Celi, R., "Steady Stall and Compressibility Effects on Hingeless Rotor Aeroelasticity in High-*g* Turns," *Proceedings of the Sixteenth Vertica*, Vol. 14, No. 4, 1990, pp. 509-531.

[15] Friedmann, P. P., and Straub, F. K., "Application of the Finite Element Method to Rotary-Wing Aeroelasticity," *Journal of the American Helicopter Society*, Vol. 25, No. 1, 1980, pp. 36-44.

[16] Rall, L. B., *Computational Solution of Nonlinear Operator Equations*, Krieger, New York, 1979, Chap. 4.

[17] Hahn, H. T., and Tsai, S. W., "Nonlinear Elastic Behavior of Unidirectional Composite Laminates," *Journal of Composite Materials*, Vol. 7, No. 1, 1973, pp. 102-118.